Available online at www.sciencedirect.com
SCIENCE DIRECT®
Biochemical and Biophysical Research Communications 323 (2004) 17–23
BBRC
www.elsevier.com/locate/ybbrc

Reverse endocytosis of transmembrane ephrin-B ligands via a clathrin-mediated pathway

Monica Parker[a], Richard Roberts[b], Miriam Enriquez[c], Xia Zhao[c], Takamune Takahashi[c], Douglas Pat Cerretti[d], Tom Daniel[c,d,1], Jin Chen[a,e,f,*]

[a] Division of Rheumatology, Department of Medicine, Vanderbilt University School of Medicine, Nashville, TN 37232, USA
[b] Department of Pathology, Department of Medicine, Vanderbilt University School of Medicine, Nashville, TN 37232, USA
[c] Division of Nephrology, Department of Medicine, Vanderbilt University School of Medicine, Nashville, TN 37232, USA
[d] Amgen Corporation, 1201 Amgen Court West, Seattle, WA 98101, USA
[e] Department of Cancer Biology, Department of Medicine, Vanderbilt University School of Medicine, Nashville, TN 37232, USA
[f] Department of Cell and Developmental Biology, Department of Medicine, Vanderbilt University School of Medicine, Nashville, TN 37232, USA

Received 28 June 2004
Available online 21 August 2004

Abstract

Eph/ephrin receptors and ligands mediate cell–cell interaction through reciprocal signaling upon juxtacrine contact, and play a critical role in embryonic patterning, neuronal targeting, and vascular assembly. To study transmembrane ephrin-B ligand trafficking, we determined the cellular localization of ephrin-B1–GFP upon engagement by EphB1. Under normal culture conditions ephrin-B1–GFP is localized to the plasma membrane, mostly at the lateral cell borders. Addition of soluble EphB1-Fc receptor induces ephrin-B1–GFP clustering on the cell surface and subsequent internalization, as judged by biochemical studies, electron microscopy, and co-localization with endosomal markers. A dominant-negative mutant of dynamin or potassium depletion blocks ephrin-B1 endocytosis. These results suggest that ephrin-B1 internalization is an active receptor-mediated process that utilizes the clathrin-mediated endocytic pathway.

Keywords: Ephrin; Endocytosis; Clathrin

Eph receptors and their cell surface-bound ligands, ephrins, mediate cell–cell recognition processes upon juxtacrine contact. They function in a variety of physiological and pathological processes in both developing and adult tissues. During embryonic morphogenesis, Eph molecules participate in axonal guidance and neural crest cell targeting, establishing rhombomere boundaries, and blood vessel remodeling [1–3]. In adult tissues, Eph molecules play an important role in tumor development and metastasis, by promoting both tumor cell invasion and recruitment of tumor blood vessels [4,5].

Eph receptors and ephrin ligands are both membrane-bound and signal bi-directionally upon engagement. The cytoplasmic and transmembrane domains of ephrin-B ligands are analogous to those of conventional receptor molecules. Similar to the receptor, ephrin-B ligands share a single transmembrane domain, a cytoplasmic region, and a C-terminal PDZ binding motif. Phosphorylation of the ephrin-B cytosolic tail leads to recruitment of a number of adapter proteins and signaling molecules [3]. Bi-directional signaling between EphB1 receptors and ephrin-B1 ligands on adjacent cells regulates in vitro endothelial cell migration and integrin-mediated cell attachment, and in vivo corneal

* Corresponding author. Fax: +1 615 343 7392.
E-mail addresses: jin.chen@vanderbilt.edu, jin.chen@mcmail.vanderbilt.edu (J. Chen).
[1] Present address: Ambrx Inc., 10410 Science Center Dr., San Diego, CA 92121, USA.

0006-291X/$ - see front matter © 2004 Elsevier Inc. All rights reserved.
doi:10.1016/j.bbrc.2004.07.209

angiogenesis [6]. Such reciprocity of signaling correlates with the developmental vascularization defects shared between mice null for ephrin-B2 [7,8] or its binding partner, EphB4 [9]. Apparent failure of anastomosis and juxtacrine EphB/ephrin-B engagement results in a reciprocal developmental arrest of the venous plexus endothelium-expressing EphB4 and the arterial plexus endothelium-expressing ephrin-B2. Furthermore, an ephrin-B2 cytoplasmic deletion mutant blocks vascular development in "knock in" mice [8], suggesting that the cytoplasmic domain of ephrin-B2 is required for transducing signals to promote neovascularization.

Bi-directional signaling through membrane-bound ligands and receptors raises the question of how these cell surface proteins are removed after ligand–receptor engagement. One mechanism by which ligand–receptor complexes from the cell surface are cleared is proteolytic cleavage. Hattori et al. [10] showed that the ectodomain of the ephrin-A2 ligand is cleaved by the metalloprotease Kuzbanian/ADAM10 in a receptor dependent manner. This cleavage is critical for separation of neuronal cells expressing the Eph receptor and fibroblasts expressing ephrin-A. Endocytosis of ligand–receptor complexes has provided an alternative mechanism to remove these proteins from the cell surface. Zimmer et al. [11] reported that EphB–ephrin-B complexes are rapidly internalized during the retraction of cells and neuronal growth cones. However, it remains unclear which endocytic pathways are involved and whether these pathways impact ephrin-B1 reverse endocytosis.

This study examines the cellular localization of ephrin-B1–GFP upon engagement by EphB1. We show here that EphB1 binding to ephrin-B1–GFP results in ephrin-B1 clustering and subsequent endocytosis. In addition, we demonstrate that ephrin-B1 internalization is inhibited by a dominant-negative dynamin mutant and potassium depletion. Together these results suggest that ephrin-B1 reverse endocytosis is mediated by a clathrin-dependent pathway. To our knowledge this is the first report directly linking ephrin-B1 reverse endocytosis with a particular endocytic pathway.

Materials and methods

Plasmids, antibodies, and reagents. Full-length cDNAs encoding ephrin-B1–GFP were constructed by inserting GFP cDNA fragments into the cytoplasmic domain of ephrin-B1 between amino acids 290 and 291. Ephrin-B1–GFP cDNA was then subcloned into the pSRα expression vector. The dominant-negative dynamin mutant (K44A) construct was generously provided by Dr. Marc Caron (Duke University). Rabbit polyclonal antibodies raised against spacer regions of ephrin-B1 and ephrin-B2 (Immunex) were used for immunoprecipitation and Western blot analyses. EphB1-Fc and EphB4-Fc were purchased from R&D system. Other primary antibodies used include mouse monoclonal against EEA1 (Transduction Laboratories) and rabbit polyclonal against caveolin (Transduction Laboratories). Secondary conjugates used were goat anti-mouse-Alexa568 (Molecular Probes), goat anti-rabbit-Alexa488 (Molecular Probes), and anti-rabbit HRP (Promega).

Cell culture, transfection, and FACS analysis. Chinese hamster ovary (CHO) cells were passaged in Dulbecco's modified Eagle's medium (DMEM) supplemented with 10% fetal bovine serum, L-glutamine, and non-essential amino acids. Primary human umbilical aortic endothelial cells (HUAECs) were passaged in ECM complete medium (Clonetics) and used up to passage 6. CHO cells were transfected using Lipofectamine Plus reagent (Gibco), either with vector alone (sRα) or plasmids expressing full-length human ephrin-B1–GFP. Cell sorting analysis of ephrin-B1 or EphB1 on the surface of CHO cells was conducted using EphB1-Fc or ephrin-B1-Fc (2 μg/ml) followed by FITC-conjugated goat anti-human IgG-Fc (Jackson Labs, 1:200). The instrument utilized was a FACS Caliber (Becton–Dickinson, San Jose, CA) using an argon ion laser at 488 nm with detection by a 530 ± 30 nm band pass filter. For dynamin mutant transfections, CHO cells were transfected using Lipofectin (Gibco), either with vector alone or the dominant-negative dynamin mutant K44A construct. To select stable clones, cells were transfected with vector or K44A plasmids along with the pCEP4 vector at a ratio of 10:1. Hygromycin resistance clones were selected in the presence of 200 μg/ml hygromycin (Gibco).

Confocal microscopy analysis. CHO-ephrin-B1/GFP cells were plated on coverslips in 6-well dishes and cultured to a 50% confluency. Growth medium was replaced with 1 ml starvation medium (DMEM + 1% BSA or Opti-MEM)/well. Four micrograms per milliliter of EphB1-Fc was added to cells and images were recorded of live cells using confocal microscopy. For co-localization studies, 0.5 μg/ml of a Texas red-labeled endosomal marker, *N*-(3-triethylammoniumpropyl)-4-(6-(4-(diethylamino)phenyl)hexathienyl)pyridium dibromide (FM 4-64) (Molecular Probes, Eugene, Oregon), was incubated with the cells at 37 °C for 20 min. This treatment was followed by stimulation with 4 μg/ml EphB1-Fc for 25 min at 37 °C. Cells were then fixed with 4% paraformaldehyde and examined under the confocal microscope. For immunofluorescence assays, cells were stimulated with 2 μg/ml EphB1-Fc for 30 min and fixed with 4% paraformaldehyde. Following fixation cells were incubated with primary (mouse anti-EEA1, 1:1000, clone 14; rabbit anti-caveolin, 1:1000, Transduction Laboratories) and secondary antibodies (Alexa568-conjugated goat anti-mouse, 1:3000, Molecular Probe). Experiments were repeated three times and more than 25 cells per experiment were analyzed.

Electron microscopy analysis. CHO-ephrin-B1/GFP cells were plated in a 12-well plate, grown to an 80% confluency, and growth medium was replaced with starvation medium (DMEM + 1% BSA). Protein A–HRP (Sigma, St. Louis, MO) and EphB1-Fc were pre-incubated in PBS for 60 min on ice (1:1). Five micrograms per milliliter of the EphB1–protein A–HRP complex or control protein A–HRP was incubated with cells for 20 min at 4 °C and followed by additional 25 min incubation at 37 °C. Cells were then fixed with 1% glutaraldehyde, stained with 3,3′-diaminobenzidine tetrahydrochloride, and analyzed by electron microscopy.

Biotinylation assay for reverse endocytosis. CHO cells or HUAECs were incubated with 0.5 mg/ml Sulfo-NHS-LC-Biotin (Piece Chemical) for 30 min at 4 °C followed by a glycine wash to quench free biotin. Cells were then incubated in normal media at 37 °C for indicated times in the presence of EphB1-Fc, EphB4-Fc, or control IgG. Biotinylated cell surface proteins were removed by 0.001% trypsinization. Remaining biotinylated proteins were sequestered inside cells by endocytosis and were therefore protected from trypsinization. Cell lysates were immunoprecipitated with anti-ephrin-B1 and biotinylated ephrin-B1 proteins were visualized by streptavidin–HRP coupled chemiluminescence detection using an ECM kit (Amersham).

Potassium (K^+) depletion. Cells were depleted of potassium to selectively block clathrin-mediated endocytosis as described by Larkin et al. [12]. Cultures were rinsed three times with K^+-free medium (20 mM Hepes, pH 7.5, 140 mM NaCl, 1 mM $CaCl_2$, 1 mM $MgSO_4$, 5.5 mM glucose, and 0.5% BSA) and incubated in the same medium

for 1 h. For confocal microscopy analysis cells were immediately stimulated with EphB1-Fc. For biochemical studies cells were surface biotinylated. Following EphB1-Fc stimulation, ephrin-B internalization was analyzed as described above. To test the effects of potassium depletion on transferrin internalization, cells were stimulated by 5 μg/ml biotinylated transferrin ligand (Sigma) and processed for confocal microscopy analysis using an avidin-Alexa 488 (1:3000; Molecular Probes) to detect internalized transferrin.

Results

Bi-directional internalization of the ephrin-B1/EphB1 complex

To reconstitute the juxtacrine contact of EphB1 and ephrin-B1 on neighboring cells in vivo, we established stable CHO cell lines that express EphB1. These cells were used as reagent "stimulators" to contact "responder" cells expressing ephrin-B1–GFP, as shown schematically in Fig. 1A (colour version online). Parental CHO cells or CHO cells expressing EphB1 were biotinylated and labeled with streptavidin–Texas red, while "responder" CHO cells express ephrin-B1–GFP (green). As shown in Figs. 1B and C, initial juxtacrine contact of EphB1-expressing cells with ephrin-B1–GFP-expressing cells induces the redistribution of ephrin-B1 to contact sites (Fig. 1B) and subsequent clustering of ephrin-B1–GFP molecules (Fig. 1C). No endocytosis was observed when control CHO cells were presented to ephrin-B1–GFP-expressing cells (Figs. 1D–F). Ephrin-B1–GFP proteins (green), however, were clearly present in CHO cells expressing EphB1 (red) (merged in Fig. 1I, yellow) when CHO/EphB1 were in contact with ephrin-B1–GFP bearing "responder" cells (Figs. 1G–I). These results suggest that the ephrin-B1 ligand stimulates EphB1 receptor internalization. Conversely, internalization of ephrin-B1–GFP (green) occurred upon contact with EphB1-expressing cells (Fig. 1I), showing internalization in the reverse direction. Taken together, these data indicate that the EphB1/ephrin-B1 complex is bi-directionally internalized upon receptor–ligand engagement. Since the GFP tag is in the cytoplasmic domain of the ephrin-B1 molecule, the presence of GFP in EphB1-expressing cells also indicates that the entire ephrin-B1 molecule is internalized into the CHO/EphB1 cells.

Reverse endocytosis of ephrin-B1 in response to EphB1-Fc stimulation

To analyze biochemically the mechanism and kinetics of ephrin-B1 reverse internalization, we utilized a soluble EphB1-Fc molecule. As the soluble receptor lacks a cytoplasmic domain, it allows us to study reverse endocytosis in the absence of all forward signaling events. Internalization of cell surface ephrin-B1 was tracked using an

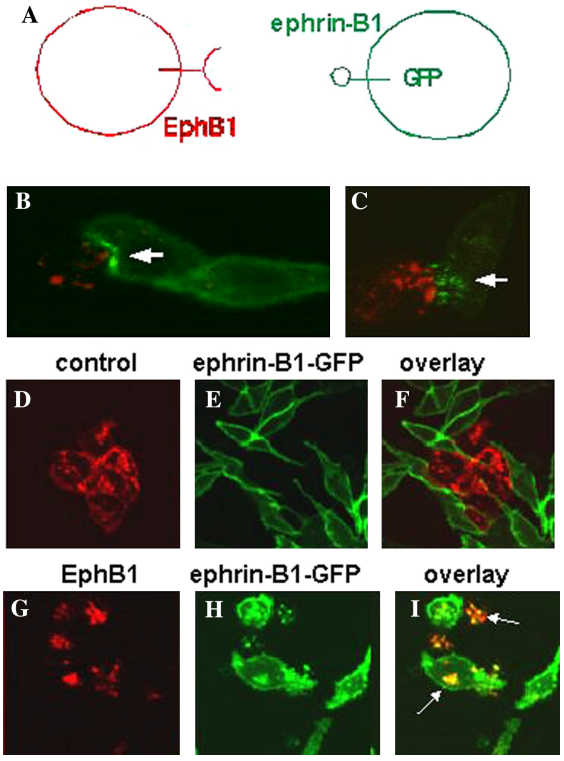

Fig. 1. Juxtacrine interaction of ephrin-B1 and EphB1 induces bi-directional endocytosis of ligand/receptor complexes. (A) Diagram of EphB1 receptor and ephrin-B1–GFP ligand as presented on CHO cells. Parental CHO cells and EphB1-expressing CHO cells were biotinylated, labeled with Texas red–streptavidin, and then presented to CHO–ephrin-B1–GFP cells. Initial juxtacrine contact of CHO/EphB1 and CHO/ephrin-B1 cells induces redistribution and clustering of ephrin-B1–GFP at the cell contact (B,C). After 4 h, while no interaction or clustering of ephrin-B1–GFP is observed with parental CHO cell presentation (D–F), ephrin-B1–GFP ligand (green) is internalized by EphB1-expressing CHO cells (red) (G–I). In the reciprocal direction, biotinylated proteins from CHO cells expressing EphB1 (red) are also internalized by CHO–ephrin-B1–GFP (green) cells (G–I). (For interpretation of the references to colors in this figure legend, the reader is referred to the web version of this paper.)

assay described by Le et al. [13]. CHO cells were surface-biotinylated at 4 °C and then returned to 37 °C following a time course to allow trafficking to resume. Cells were then incubated briefly with a dilute trypsin solution to remove cell surface proteins. Internalized ephrin-B1 was sequestered at 37 °C and therefore protected from trypsin digestion. No ephrin-B1 was detected in control cells (Fig. 2A, 0 min), confirming that under these conditions biotinylated cell surface proteins were efficiently removed by trypsin. In contrast, after 10 and 30 min at 37 °C a biotinylated pool of ephrin-B1 was detected in cells following trypsin treatment (Fig. 2A, 10 and 30 min), indicating that ephrin-B1 was internalized and protected from typsinization. Both EphB1-Fc and control treatment induced ephrin-B1 internalization, but the level of internalized ephrin-B1 was appreciably higher in EphB1-Fc-stimulated cells compared to that in con-

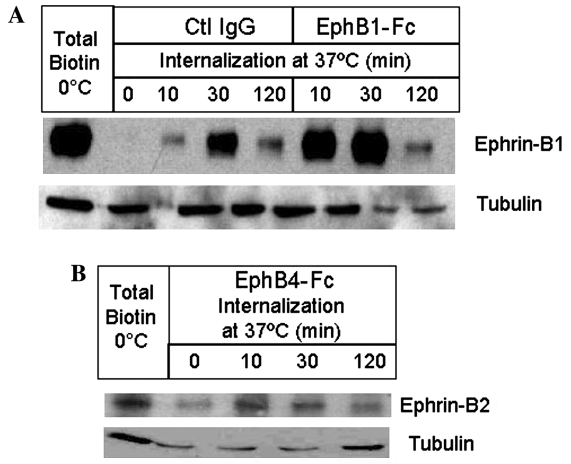

Fig. 2. EphB1-Fc stimulates ephrin-B1 reverse internalization. Biochemical studies were performed using a soluble EphB1-Fc molecule to study reverse endocytosis. Cells were biotinylated and surface proteins were either removed immediately as indicated by the 0 time point or removed following a time course of EphB/Fc stimulation. Levels of internalized ephrin-B were then determined by IP-Western blot analysis. Ephrin-B1–GFP was internalized following 10 and 30 min of EphB1-Fc stimulation (A). Endothelial cells expressing endogenous ephrin-B2 exhibited maximum internalization at 10 min following EphB4-Fc stimulation (B).

trol treated cells (Fig. 2A). To determine whether endogenous ephrin-B is endocytosed, we biotinylated ephrin-B2-expressing human umbilical arterial endothelial cells (HUAECs) followed by stimulation with EphB4-Fc to analyze endocytosis. As shown in Fig. 2B, EphB4-Fc induced internalization of ephrin-B2 at 10 and 30 min, consistent with results obtained from CHO/ephrin-B1 cells. These data indicate that a certain portion of ephrin-B1 is constitutively internalized. Receptor stimulation, however, increases the level and kinetics of ephrin-B1 internalization.

Using confocal microscopy, we characterized the subcellular localization of ephrin-B1 following internalization. In un-stimulated cells, ephrin-B1–GFP appears as a diffuse population around the cell boarders (Fig. 3A). Upon stimulation with soluble EphB1-Fc, ephrin-B1–GFP clusters rapidly and localizes in large patches (Fig. 3B), followed by internalization of ephrin-B1 (Fig. 3C, yellow). These internalized vesicles were co-stained with FM4-64, a membrane dye (Fig. 3C, arrow; colour version online), confirming that ephrin-B1 is internalized during reverse signaling.

As a complementary approach, we studied the localization of internalized EphB1–ephrin-B1 complex using electron microscopy. EphB1-Fc or control IgG was incubated with protein A to form EphB1-Fc–protein A or IgG–protein A complexes, respectively. Ephrin-B1–GFP-expressing CHO cells were stimulated with either control IgG–protein A or EphB1-Fc–protein A complexes for 25 min, fixed, and processed for diaminobenzidine (DAB) cytochemistry and electron microscopy. In contrast to ephrin-B1–GFP cells stimulated with IgG–protein A (Fig. 3D), cells exposed to the EphB1-Fc–protein A–HRP complex showed a large number of intracellular vesicles that exhibited strong DAB staining (Figs. 3E and F). Together these results show that upon EphB1 stimulation ephrin-B1 is internalized to intracellular vesicles.

We next assessed the nature of these intracellular vesicles by confocal microscopy using the early endosomal marker, EEA1 [7,19], or the lipid raft marker caveolin [5]. As shown in Fig. 4A (colour version online), control IgG does not induce ephrin-B1–GFP/EEA1 (red) co-localization. In contrast, when cells were stimulated with EphB1-Fc, we observed significant levels of ephrin-B1–GFP/EEA1 co-localization (yellow in overlay panel), suggesting that EphB1-Fc induces ephrin-B1 internali-

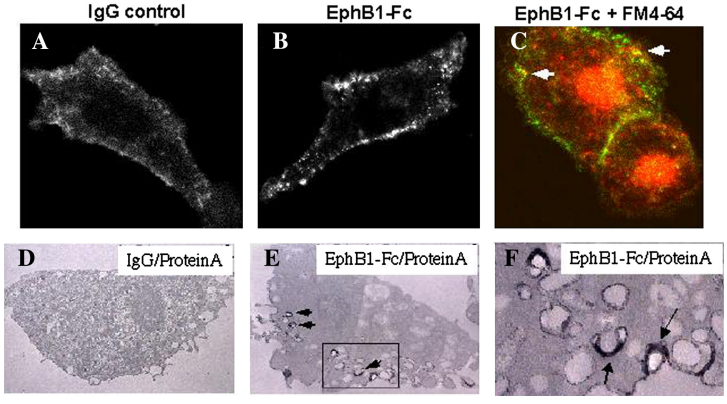

Fig. 3. EphB1-Fc stimulates ephrin-B reverse internalization into intracellular vesicles (colour version online). Ephrin-B1–GFP is localized diffusely at the cell boarder when stimulated by control IgG (A); while EphB1-Fc stimulation results in ephrin-B1 clustering and internalization (B). Limited internalization of ligand–receptor complexes is observed based on co-localization with the membrane dye, FM4-64 (C). For electron microscopy experiments, CHO cells expressing ephrin-B1 were stimulated for 25 min at 37 °C with a complex of peroxidase-conjugated protein A–IgG or -EphB1-Fc, and stained with DAB. IgG/protein A–HRP complex was not internalized (D). EphB1-Fc–protein A–HRP complex appears to localize to intracellular vesicles, as indicated by arrows (E). Higher magnification of the boxed area in (E) reveals more clearly this vesicular localization (F).

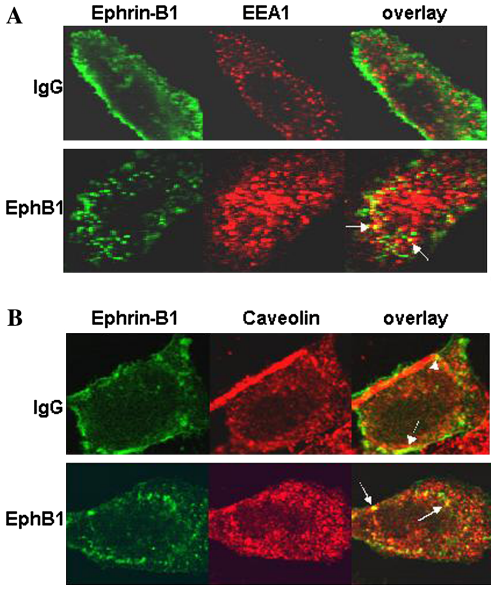

Fig. 4. Soluble EphB1-Fc induces ephrin-B1–GFP co-localization with EEA1 (colour version online). (A) By confocal microscopy co-localization of ephrin-B1 and the early endosomal marker, EEA1, was assessed. In CHO–ephrin-B1–GFP cells that were control (Ctl) stimulated little to no co-localization with EEA1 was observed. EphB1-Fc (EphB1) stimulation induced clustering and ephrin-B1/EEA1 co-localization. (B) By confocal microscopy co-localization of ephrin-B1 and the lipid raft marker, caveolin, was assessed. Both control (Ctl) and EphB1-Fc (EphB1) stimulated CHO–ephrin-B1–GFP cells displayed caveolin co-localization.

zation into early endosomal vesicles. For caveolin staining, we observed co-localization of ephrin-B1 with caveolin in both control and EphB1-Fc-stimulated cells (Fig. 4B), indicating that ephrin-B1 may constitutively reside in raft microdomains irrespective of receptor stimulation.

Blocking of the clathrin-mediated pathway inhibited ephrin-B1 reverse endocytosis

Ephrin-B1 was previously reported to reside in membrane microdomains enriched in glycolipids and cholesterol, called rafts [14], a result consistent with the co-localization of ephrin-B1 and caveolin in the present study. However, the ephrin-B1 cytoplasmic tail contains a putative tyrosine-based sorting signal, YXXϕ. Adapter protein (AP) complexes utilize this signal to select cargo for inclusion into coated vesicles in order to regulate clathrin endocytosis [15]. Based on this finding and the fact that we were unable to detect significant changes in ephrin-B1 endocytosis by blocking the caveolae-mediated pathway, we focused on studies to determine whether receptor-stimulated ephrin-B1 internalization is clathrin-dependent.

To accomplish this task, we utilized a dominant-negative dynamin (K44A) to block endocytosis. Dynamin is a GTPase required for the release of clathrin-coated pits (reviewed in [16,17]). Stable CHO clones expressing parental vector control or K44A dynamin were transiently transfected with ephrin-B1–GFP and stimulated with control protein or EphB1-Fc. Co-localization of the endosomal marker EEA1 and ephrin-B1–GFP was analyzed by confocal microscopy. Control treatment of both vector and K44A-expressing cells did not induce ephrin-B1–GFP/EEA1 co-localization (Figs. 5A and B). In vector-expressing cells EphB1-Fc treatment induced ephrin-B1 endocytosis (Fig. 5C). Cells expressing the K44A dynamin mutant protein, however, exhibited diminished ephrin-B1–GFP/EEA1 co-localization (Fig. 5D). These results support the notion that ephrin-B1 is internalized via a clathrin dependent endocytosis pathway.

Recent studies suggested that caveolae-mediated endocytosis is also dynamin-dependent [18]. To specifically inhibit clathrin-coated pit formation, we used potassium depletion which blocks clathrin-cage assembly [12]. Cells were pretreated with minimal media that either contained potassium or was devoid of potassium. Following this pretreatment, cells were stimulated at 37 °C to induce internalization. In control experiments transferrin was utilized to demonstrate the ability of potassium depletion to block clathrin-mediated endocytosis. Consistent with prior studies [19], potassium depletion blocked transferrin internalization (Fig. 6A).

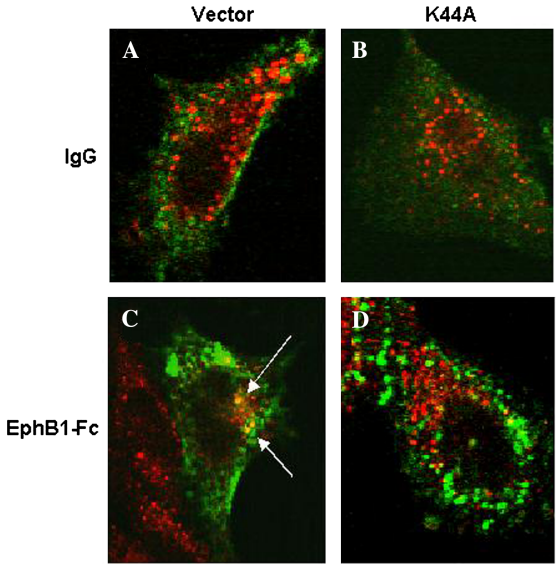

Fig. 5. Dynamin mutant expression diminishes EphB1-Fc-induced ephrin-B1 clustering and internalization (colour version online). CHO cells stably transfected with the parental vector (vector) were transiently transfected with ephrin-B1–GFP. As expected, stimulation of these cells with control IgG had no effect on ephrin-B1/EEA1 co-localization (A,B). EphB1 stimulation of vector control expressing CHO cells induced ephrin-B1/EEA1 co-localization (C), while EphB1 stimulation of CHO cells stably expressing a dominant-negative dynamin construct (K44A) did not induce ephrin-B1/EEA1 co-localization (D).

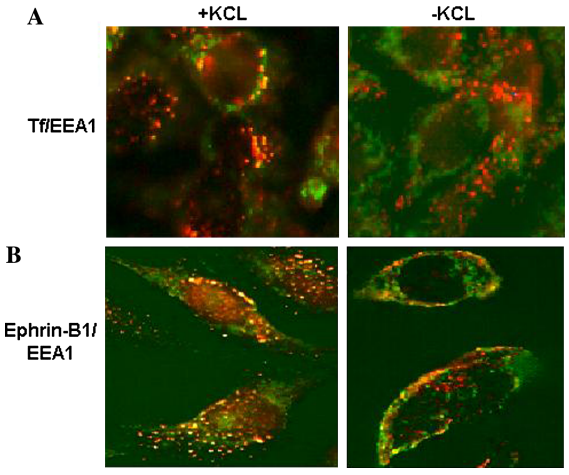

Fig. 6. Potassium depletion inhibited ephrin-B1 clustering and internalization (colour version online). (A) Potassium depletion greatly diminishes transferrin internalization as judged by decreased EEA1 co-localization. (B) Similarly, EphB1-Fc stimulation of ephrin-B1 clustering and internalization is attenuated under conditions of depleted potassium.

As shown in Fig. 6B, EphB1-induced ephrin-B1 internalization was also greatly inhibited by potassium depletion. Taken together, these results suggest that the clathrin-mediated endocytic pathway plays a critical role in EphB1-induced ephrin-B1 reverse internalization.

Discussion

Receptor tyrosine kinases (RTKs) mediate cell–cell interaction and play an important role in controlling many fundamental cellular processes including cell proliferation, differentiation, migration, and survival [20]. Consequently, the activity of RTKs must be tightly regulated in order to mediate their normal cellular tasks and many physiological responses. Rapid internalization of activated RTKs through ligand-induced endocytosis was traditionally thought to be one of the mechanisms to attenuate signal transduction. In this report, we provide direct evidence that [1] the EphB1/ephrin-B1 complex is internalized bi-directionally upon juxtacrine contact of cells expressing the ligand and receptor, [2] stimulation of ephrin-B1-expressing cells using a soluble EphB1-Fc molecule induces a rapid increase in reverse endocytosis of ephrin-B1 to intracellular endosomes, and [3] ephrin-B1 reverse internalization is mediated by a clathrin-dependent pathway.

The majority of RTKs are activated by soluble ligands. Ligand binding induces receptor clustering on the cell surface, followed by internalization into intracellular vesicles. This often leads to lysosomal degradation or recycling back to the cell membrane [21–24]. It is less clear, however, what happens to RTKs that are activated by membrane-bound ligands. In principle, membrane-bound ligands could be cleaved by proteases and then internalized by receptor-mediated endocytosis. Indeed, Eph receptor binding triggers ephrin-A2 cleavage by the metalloprotease Kuzbanian in neuronal cells [10]. However, we do not observe cleavage of ephrin-B1 upon EphB1 binding in our experimental system. Instead, we observe ephrin-B1–GFP molecules in both ephrin-B1-expressing cells and the Texas red-labeled EphB1 receptor-expressing cells (Fig. 1, yellow dots in I). As the GFP tag is on the cytoplasmic domain of ephrin-B1, these results suggest that the entire molecule of ephrin-B1 is internalized upon binding to the cell-surface EphB1 receptor. These results are consistent with recent reports of Eph/ephrin internalization induced neuronal growth cone retraction [11,25]. The EphB/ephrin-B complex is bi-directionally endocytosed in a manner that comprises full-length receptor and ligand complexes.

Vesicular trafficking or endocytosis is essential to the regulation of the entry of small and large molecules. Endocytosis occurs via several mechanisms [21]. The best understood mechanism involves the formation of a cytoplasmic clathrin coat. Molecules going through clathrin-mediated pathway usually contain an endocytosis signal YXXϕ, a sequence that is recognized by the clathrin-associated adapter proteins required for loading molecules into clathrin-coated pits and vesicles. More recently, lipids are also recognized as very important in the internalization process. In particular, caveolae-mediated endocytosis has been shown to mediate the turn over of several receptors [26,27]. Previous studies have reported localization of ephrin-B1 to the rafts-cholesterol rich plasma membrane microdomains [14]. Although we also observed the co-localization of caveolin and ephrin-B1 in EphB1-Fc-stimulated cells, ephrin-B1 reverse endocytosis does not appear to be affected by blocking caveolae-mediated endocytosis (data not shown). In contrast, our data support the involvement of the clathrin-mediated pathway in ephrin-B1 reverse endocytosis. First, the C-terminal portion of ephrin-B1 encodes a putative clathrin internalization signal, and internalized ephrin-B1 is co-localized with EEA1, an endosomal marker. Furthermore, two independent means to block the clathrin-mediated pathway, a dominant-negative dynamin mutant, K44A, and potassium depletion, inhibited internalization of ephrin-B1 upon EphB1-Fc stimulation. To our knowledge this is the first report directly linking ephrin-B1 reverse endocytosis with a particular endocytic pathway.

Endocytosis of ligand-activated receptors has traditionally been considered a mechanism to attenuate or terminate signaling. However, a growing body of evidence suggests an emerging pattern of endocytic membrane trafficking and intracellular signaling [28]. Both clathrin-mediated and caveolae-mediated endocytic pathways have been implicated in regulating the inten-

sity of signaling and the co-localization of activated receptor with downstream signaling molecules [14,26,29,30]. It remains to be determined whether ephrin-B1 reverse endocytosis serves to down-regulate surface receptor level or mediates cellular signaling events. Thus, our results provide a basis for additional studies of intracellular trafficking of ephrin-B1.

Acknowledgments

We thank Amanda Kizzee for excellent technical assistance, and Drs. Anne Kenworthy and Dana Brantley-Sieders for helpful discussions and comments on the manuscript. This work was supported by National Institutes of Heath Grants DK47078 and CA95004 to J. Chen, and an NRSA postdoctoral fellowship F32 HL74517-01 to M. Parker. This work was also supported by the Vanderbilt Cancer Center imaging core, and a core facility Grant 2P30CA68485 to the Vanderbilt-Ingram Cancer Center.

References

[1] N. Holder, R. Klein, Development 126 (1999) 2033–2044.
[2] J.G. Flanagan, P. Vanderhaeghen, Annu. Rev. Neurosci. 21 (1998) 309–345.
[3] N. Cheng, D. Brantley, J. Chen, Cytokine Growth Factor Rev. 13 (2002) 75–85.
[4] M. Nakamoto, A. Bergmann, Microsc. Res. Techn. 59 (2002) 58–67.
[5] D.M. Brantley, N. Cheng, E.J. Thompson, Q. Lin, R.A. Brekken, P.E. Thorpe, R.S. Muraoka, D.P. Cerretti, A. Pozzi, D. Jackson, C. Lin, J. Chen, Oncogene 21 (2002) 7011–7026.
[6] U. Huynh-Do, C. Vindis, H. Liu, D.P. Cerretti, J.T. McGrew, M. Enriquez, J. Chen, T.O. Daniel, J. Cell Sci. 115 (2002) 3073–3081.
[7] H.U. Wang, Z.F. Chen, D.J. Anderson, Cell 93 (1998) 741–753.
[8] R.H. Adams, F. Diella, S. Hennig, F. Helmbacher, U. Deutsch, R. Klein, Cell 104 (2001) 57–69.
[9] S.S. Gerety, H.U. Wang, Z.F. Chen, D.J. Anderson, Mol. Cell 4 (1999) 403–414.
[10] M. Hattori, M. Osterfield, J.G. Flanagan, Science 289 (2000) 1360–1365.
[11] M. Zimmer, A. Palmer, J. Kohler, R., Klein, Nat. Cell Biol. 5 (2003) 869–878.
[12] J.M. Larkin, M.S. Brown, J.L. Goldstein, R.G.W. Anderson, Cell 33 (1983) 273–285.
[13] T.L. Le, A.S. Yap, J.L. Stow, J. Cell Biol. 146 (1999) 219–232.
[14] K. Bruckner, J.P. Labrador, P. Scheiffele, A. Herb, P.H. Seeburg, R. Klein, Neuron 22 (1999) 511–524.
[15] L.M. Traub, J.S. Bonifacino, Annu. Rev. Biochem. 72 (2003) 395–447.
[16] S.M. Barbas, L.J. Terlecky, K. Tang, S. Hardy, K.E. Mostov, S.L. Schmid, J. Cell Biol. 143 (1998) 1871–1881.
[17] J.E. Hinshaw, Curr. Opin. Cell Biol. 13 (2001) 454–460.
[18] J.R. Henley, E.W. Krueger, B.J. Oswald, M.A. McNiven, J. Cell Biol. 141 (1998) 85–99.
[19] S.H. Hansen, K. Sandvig, B. van Deurs, J. Cell Biol. 113 (1991) 731–741.
[20] J. Schlessinger, Cell 103 (2000) 211–225.
[21] S.D. Conner, S.L. Schmid, Nature 422 (2003) 37–44.
[22] M.D. Marmor, Y. Yarden, Oncogene 23 (2004) 2057–2070.
[23] J.F. Presley, S. Mayor, T.E. McGraw, K.W. Dunn, F.R. Maxfield, J. Biol. Chem. 272 (1997) 13929–13936.
[24] J. Walker-Daniels, D.J. Riese, M.S. Kinch, Mol. Cancer Res. 1 (2002) 79–87.
[25] D.J. Marston, S. Dickinson, C.D. Nobes, Nat. Cell Biol. 5 (2003) 879–888.
[26] G.M. Di Guglielmo, C. Le Roy, A.F. Goodfellow, J.L. Wrana, Nat. Cell Biol. 5 (2003) 410–421.
[27] P. Oh, J.E. Schnitzer, Mol. Biol. Cell 12 (2001) 685–698.
[28] B.P. Ceresa, S.L. Schmid, Curr. Opin. Cell Biol. 12 (2000) 204–210.
[29] H. Gicquiaux, S. Lecat, M. Gaire, A. Dieterlen, Y. Mely, K. Takeda, B. Bucher, J.L. Galzi, J. Biol. Chem. 277 (2002) 6645–6655.
[30] A.V. Vieira, C. Lamaze, S.L. Schmid, Science 274 (1996) 2086–2089.